Iridium-Based Hydride Transfer Catalysts: from Hydrogen Storage to Fine Chemicals

Journal:	*ChemComm*
Manuscript ID	CC-FEA-04-2018-003412.R1
Article Type:	Feature Article

Chemical Communications

Feature Article – Referee Guidelines

A *ChemComm* Feature article is not a typical review. It is meant to highlight the authors' contribution to a growing area, bringing together their key results, while presenting a balanced discussion of related work to set the authors' contribution within a wider context.

While there are no strict guidelines on the writing style, a Feature article should generally include:

- A background to the research area; its importance and previous developments
- A summary of the key aspects of the research recently published by the author
- An outlook on future progression of the field, including how the author's research could impact that.

When reviewing a Feature article please bear in mind the journal's broad readership. It is essential that Feature articles are clearly written, up-to-date, authoritative and easily comprehensible to the non-specialist, and that they do not overlap with any other published or planned review.

Feature Articles should ideally be between 10 and 16 pages in length, although longer articles may be acceptable after consultation with the Editorial Board.

Thank you very much for your assistance in evaluating this manuscript.

General Guidance

Referees have the responsibility to treat the manuscript as confidential. Please be aware of our **Ethical Guidelines**, which contain full information on the responsibilities of referees and authors, and our **Refereeing Procedure and Policy**.

When preparing your report, please:

- comment on the significance, impact and scientific reliability of the work;
- state clearly whether you would like to see the article accepted or rejected and give detailed comments (with references, as appropriate) that will both help the Editor to make a decision on the article and the authors to improve it.

Please inform the Editor if:

- there is a conflict of interest;
- there is a significant part of the work which you are not able to referee with confidence.

Submit your report at http://mc.manuscriptcentral.com/chemcomm

Journal Name

FEATURE

Iridium-Based Hydride Transfer Catalysts: from Hydrogen Storage to Fine Chemicals

Received 00th January 20xx,
Accepted 00th January 20xx

DOI: 10.1039/x0xx00000x

www.rsc.org/

Zhiyao Lu, Valeriy Cherepakhin, Ivan Demianets, Paul J. Lauridsen, and Travis Williams*[a]

Abstract: Selective hydrogen transfer remains a central research focus in catalysis: hydrogenation and dehydrogenation have central roles, both historical and contemporary, in all aspects of fuel, agricultural, pharmaceutical, and fine chemical synthesis. Our lab has been involved in this area by designing homogeneous catalysts for dehydrogenation and hydrogen transfer that fill needs ranging from on-demand hydrogen storage to fine chemical synthesis. A keen eye toward mechanism has enabled us to develop systems with excellent selectivity and longevity and demonstrate these in a diversity of high-value applications. Here we describe recent work from our lab in these areas that are linked by a central mechanistic trichotomy of catalyst initiation pathways that lead highly analogous precursors to a diversity of useful applications.

1. Introduction

Hydrogen transfer is one of the historically most developed and most useful applications of homogeneous catalysis and remains a very fruitful area of active investigation today,[1–8] and many important advancements have been made in the field in recent years.[9-33] Dehydrogenation is a major frontier of this enterprise, with well-established dehydrogenation of alkanes to olefins and alcohols to carbonyl compounds among important examples of such transformations. Hydrogen produced in these reactions has utility as a carbon-free energy carrier,[34–37] but mastery of hydrogen fuel will require improved methods for its weight-efficient, reversible storage on liquid media, which in turn, motivates further work in hydrogen transfer catalysis. Such developments in catalysts lead to high-value new reactions that have utility in all areas of synthesis, including fuel upgrading, fine chemicals, and even complex molecule synthesis.

This feature will highlight a recent project of our lab in which we set out to discover useful catalysts for hydrogen release from small-molecule hydrogen carriers.[38] The work led us to a family of iridium hydride clusters and related organometallics that have utility in on-demand hydrogen generation, fine chemicals synthesis, biofuels, and complex molecules, with each application arising from distinct, related derivatives of highly analogous catalyst precursors that differentiate themselves through intricate catalyst initiation pathways. Here we will summarize the context and application of these new catalytic reactions and advance, for the first time, a unifying hypothesis of how subtly different influences in catalyst initiation govern the capability of the initiated catalysts.

1.1 Catalytic release of stored hydrogen

Hydrogen has a high energy content (120 MJ/kg) that exceeds that of gasoline by almost three times (44 MJ/kg),[39] therefore it is well suited for chemical energy storage.[40] It can either be burned in an engine or oxidized in a fuel cell to produce electricity. In both cases, water is the only by-product, providing clean, carbon-free energy storage. Moreover, vehicles powered by hydrogen fuel cells have other advantages such as silent operation and higher efficiency, making them particularly desirable for urban communities.[41]

Large scale utilization of hydrogen as a fuel is challenging, since it is a gas at ambient conditions. Compression, cryogenic liquefaction, and absorption are among available hydrogen storage strategies, however all of these are known to have undesirable cost, capacity, and safety issues.[42] Dehydrogenation of small molecules is an attractive approach to on-demand hydrogen release. Organic hydrogen carriers like formic acid or methanol have high hydrogen storage density and can be distributed by existing fuel infrastructure. Furthermore, selective dehydrogenation of these compounds would result in only hydrogen and carbon dioxide. The latter can then be recycled by known systems,[43–45] fulfilling a carbon-neutral fuel cycle.

Today there are many heterogeneous[46,47,56,57,48–55] and homogeneous[58,59,68–74,60–67] systems for catalytic formic acid dehydrogenation. Heterogeneous catalysts are known to be reusable and easily separable from the reaction mixture.[54] However, these often require forcing conditions and afford poor selectivity. Homogeneous catalysts are typically more efficient and selective, but have longevity and recovery costs that make them impractical. Selectivity is a crucial issue:

carbon monoxide is a common side product of formic acid decomposition, and a small amount of is known to poison fuel cells, thus disqualifying unselective catalysts from this use. Therefore, studies that help define the origin of selectivity and give us structural insight into how formic acid and methanol dehydrogenation catalysts work have value in our ability to realize practical solutions to on-demand hydrogen release in a C1 fuel cycle.

1.1 Glycerol utilization

Glycerol oxidation is an example of alcohol dehydrogenation that has important similarities to the C1 dehydrogenation problem above. The most important of these similarities is scale: glycerol production is growing rapidly, because glycerol is a 10 wt% by-product of biodiesel production. Biodiesel production has grown to 2.1 billion gallons annually in the U.S. alone in 2017.[75] Since there are no convenient ways to use or dispose glycerol, this is creating a glut of this highly-functionalized C3 fragment in the global market. Thus, many excellent catalytic methods have appeared in which glycerol is converted to value-added materials like glycols or fine chemicals.[76–81] Our favorite among these products is lactic acid, although like formic acid to hydrogen, this glycerol to lactic acid is another example of a reaction made impractical by low selectivity: even when lactate is the major product in this transformation, small portions of glycols are usually formed. These inhibit the thermal oligomerization of lactic acid that is needed for its conversion to the lactide monomers used in poly(lactic acid) synthesis. With the rapidly growing market for biodegradable plastics[82] and low efficiency of fermentation-based lactic acid production, the major source of lactate today, selective glycerol-based technology has great value.

2. Reaction & Mechanism Data

In this section we will summarize several dehydrogenative reactions of high utility and intriguing mechanism that have emerged from our group in the last two years. The first is formic acid dehydrogenation by iridium precursor **1** (Figure 1). We took on this reaction, because it has potential utility in on-demand hydrogen evolution and energy generation. Despite a lower hydrogen storage density (4.4 wt%) than methanol (12.6 wt%), formic acid has important advantages: first, it is a potential solar fuel, because H_2 can be generated from solar-driven water splitting and efficient synthesis of formic acid from CO_2 and H_2 is known.[43,68,91–94,83–90] Further, formic acid and its spent fuel by-products are environmentally benign. The corrosivity of formic acid makes its dehydrogenation very difficult to achieve in the absence of high loadings of solvent or base, so we saw an opportunity to introduce the first system for dehydrogenation of neat formic acid, with the hope that understanding the mechanism of such a reaction could teach valuable lessons on how to create catalysts that are robust and selective in these challenging conditions.

2.1 Iridium based formic acid dehydrogenation

Complex **1**, prepared from $[Ir(COD)Cl]_2$, was designed by our group as a hydrogenation catalyst (Figure 1).[95] The design was based on our hypothesis that the P—N ligand in **1** can be deprotonated in basic media and then serve as part of an H_2-activation system, analogous to those developed by Milstein.[96] We rapidly learned that although such an H_2 cleavage mechanism was plausible, complex **1** was much less reactive in the reduction direction than it is in dehydrogenation, and that **1** is among the most prolific formic acid dehydrogenation catalysts known. The weak basicity of the optimized catalytic conditions does not deprotonate the P—N ligand as it mediates this catalysis.

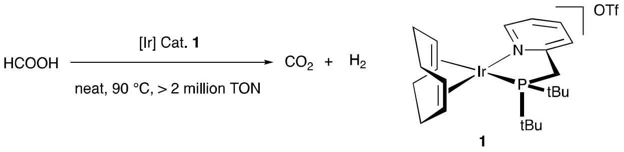

Figure 1. Formic acid dehydrogenation by iridium complex **1**.

The reaction in figure 1 has several very practical features. First, iridium precursor **1** forms a robust, prolific catalytic species that enables useful turnover frequency (average TOF 0.82 s^{-1}, maximum TOF 3.7 s^{-1}) through more than 2 million turnovers. Second, the catalyst is easy to use and reuse. The setup comprises simply mixing the reaction components in a reactor, heating to the desired temperature, and venting and collecting the gaseous products: no measures are needed to exclude air or water. In our lab, we have successfully reused the catalyst for 50 charges seeing only marginal loss in reactivity. Third, the catalyst is highly selective. In our optimized conditions, CO evolution is limited below our CO detection limit (10 ppm). Lastly, the reaction works in neat, technical grade formic acid with no purification or pre-treatment. This last fact is vital for this technology to be applied outside the lab. Obviating the need for any solvent increases the amount of energy per mass of fuel, and air and water tolerance mitigates many logistical hurdles.

We probed the mechanism of our formic acid dehydrogenation by first attempting directly to observe catalyst initiation, which gave us a good structural starting point (Scheme 1). Treating precatalyst **1** with conditions similar to the catalytic conditions, but at lower temperatures, enabled us to see a stepwise catalyst initiation. The first observable step is hemi-reduction of the COD ligand, which is dissociated from the complex as cyclooctene. This is then further reduced to cyclooctane at a slower rate. We can observe an intermediate in this reduction, **2**, under similar reducing conditions, such as H_2 or alkoxide. We propose a short-lived iridium hydride species (such as **3**) that quickly dimerizes to afford intermediate **4**, a long-lived, binuclear iridium species with two bridging and two terminal hydrides. Although analogous, **4**-like structures are commonly observed in iridium-catalyzed hydrogenations,[97] **4** does not persist after our catalytic reaction starts. In fact, isolated catalytic species from the dry, solid substance that remains after a catalytic run comprises a mixture of **5** and **6**. The structure of intermediate **5** was confirmed crystallographically by independent synthesis of its more stable acetate congener. These studies gave us reliable structural proposals for materials **1**, **2**, **4**, and **5** and authenticated **5** and **6** as the resting states of the active catalyst.

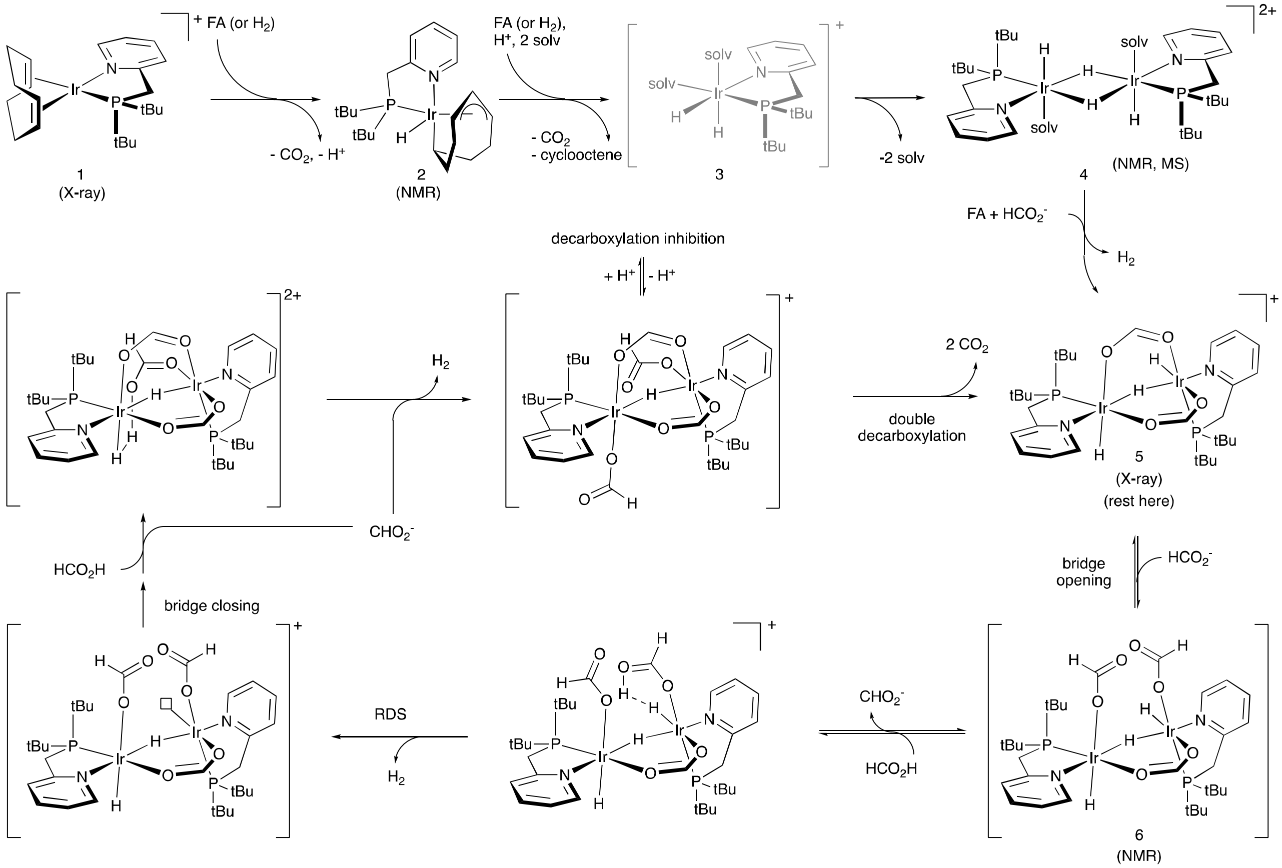

Scheme 1. Proposed mechanism for formic acid dehydrogenation by iridium precatalyst **1**.

Kinetic experiments were done to evaluate the roles of each component in the reaction and to understand the relationships of the observable species in the catalysis. The reaction is first order in iridium, which indicates that the active species is robust throughout the cycle. We observe half order dependence on the formate co-catalyst, which we interpret to indicate that a single formate is generating two active sites on the catalyst with each cycle. Further, when the reaction is diluted in tetraglyme, we see first-order inhibition of catalysis by formic acid, which we understand to indicate that acid drives the **5**/**6** equilibrium backwards.

The observation of half order dependence on formate is perplexing, however, it is quite possible with **5**. There are two formate bridges in **5**, each presenting a possible reaction site. One formate can activate a formate bridge, demonstrated in the conversion **5** to **6**. The formate can be regenerated by deprotonating formic acid, activating the other formate bridge, thus setting up the other reactive site for H_2 release. In doing so, one formate enables two turnovers. Another reasonable interpretation of this half order dependence is a radical chain mechanism, but we disfavor such a path because the rate of catalysis is not modified by radical inhibitors like BHT. Further, we think that the exclusive selectivity against CO formation is inconsistent with a radical chain. We are continuing to probe this issue.

Kinetic isotopic studies show significant isotopic effects in both the C–H (3.8) and the O–H (1.7) of formic acid, indicating that both C–H and O–H are involved in or before the rate determining step in the catalytic cycle. The product of C–H and O–H KIEs equals the overall CHOH/CDOD KIE (6.5), which indicates involvement of both C–H and O–H in a single rate determining step. Moreover, H-D crossover experiments show perfect C–H/O–H fidelity. These data point to an hypothesis that the rate determining step may be protonation of an iridium hydride to evolve H_2, where the iridium hydride originates from decarboxylation of a formate.

Rather remarkably, none of the many known congeners of **4** engage in the twisting rearrangement necessary form **5**, which might explain why **5**'s reactivity was not reported prior to our discovery. It is also interesting that, while multi-metallic formate clusters are known to form bridges when treated with acid,[98] even neat formic acid does not effectively block the conversion of **5** to **6**, thus enabling catalysis to continue.

2.2 Iridium based glycerol dehydrogenation

Glycerol has historically been an important industrial material that, in prior years, was made in its own production facilities.[99] This situation has changed with the rapid growth of biodiesel production. Glycerol accounts for ca. 10% the total mass of vegetable oils, the raw material for biodiesel production. Increasing biodiesel production has led to an oversupply of glycerol, and in some places it had become common practice to dump glycerol into water streams as a light pollutant.[99] This is a huge waste. By our calculation, disposing glycerol waste accounts for nearly 10% of the total cost in biodiesel production. Such environmental damage and economic loss is foreseeably going to exacerbate as global biodiesel production has been ramping up at a rate of 14.1% per year.[100]

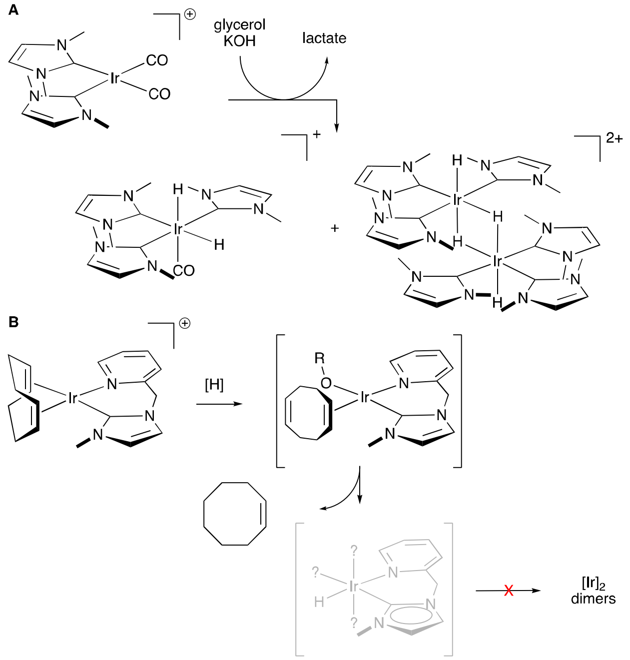

Scheme 2. **A.** Decomposition of Crabtree's di(carbene)iridium catalysts. **B.** Pyridine-supported carbenes should not deactivate in a similar way.

Catalytic conversion of glycerol to lactic acid is known with several conditions,[101–106] but selectivity remains an issue with many of them. Our entry into this reactions was designed from an observation by Crabtree that his di(carbene)iridium catalysis have good selectivity (ca. 95%), and deactivates by carbene exchange (Scheme 2). We reasoned that if a di(carbene)iridium precursor deactivates as a tri(carbene)iridium dihydride product, there must be a mono(carbene)iridium species in the reaction, and, since it is not observed, it is likely to be reactive. We determined therefore to prepare a mono(carbene)iridium species in which the carbene ligand was chelated to the metal with a supporting pyridine fragment. We hoped that this would reduce what appears to be a 3-catalyst problem to a 1-catalyst system and enable higher selectivity.

Iridium complexes **1**, **5**, and **7**-**9** were synthesized (Figure 2) and tested in reactions with neat glycerol.[107] In the presence of sodium or potassium hydroxide at typically 120-145 °C, **7**, **8** and **9** proved to be exceptionally selective in dehydrogenating glycerol to lactate – no other product was observed in ^{1}H-NMR. This selectivity is important, because in most glycerol dehydrogenation reactions, by-products that are similar in physical properties make it very costly to isolate the desired lactic acid.[108,109] Iridium complex **1** also oxidizes glycerol at a fast rate but with unusable selectivity. Curiously, despite being a reactive intermediate in formic acid dehydrogenation, **5** is ineffective in glycerol oxidation. This is evidence that the reactive species of alcohol oxidation by **1** is different than **5**.

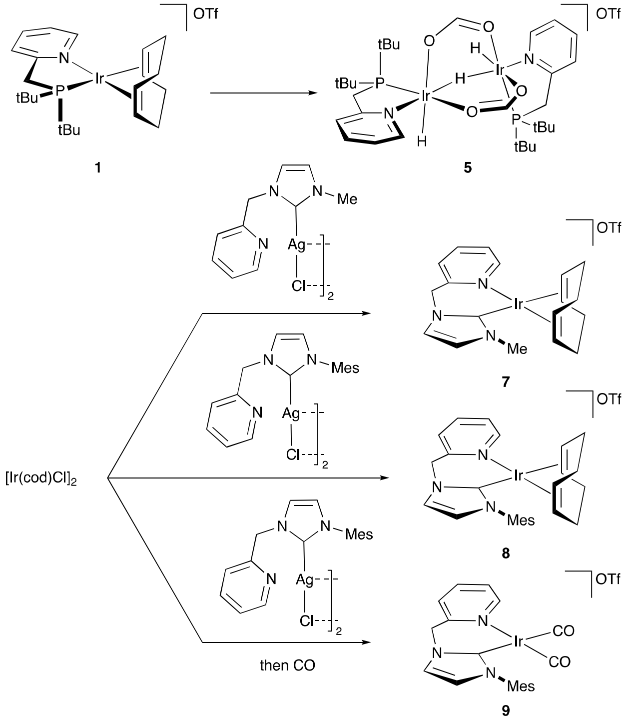

Figure 2. Synthesis of iridium complexes **7**-**9**.

Utility studies show that iridium precatalyst **7** enables a glycerol dehydrogenation system that is both fast and robust. Up to 4.56 million turnovers were observed and up to $4x10^4$ h^{-1} TOF was measured at 145 ^oC. In a typical run, **7** can convert > 90% glycerol to lactate, and the reaction then slows down as the reaction solidifies as an ionic solid. The catalyst is stable to impurities in the glycerol stream, moreover even common catalytic poisons (e.g. 1,10-phenanthroline, triphenylphosphine) have no impact on the reaction kinetics.

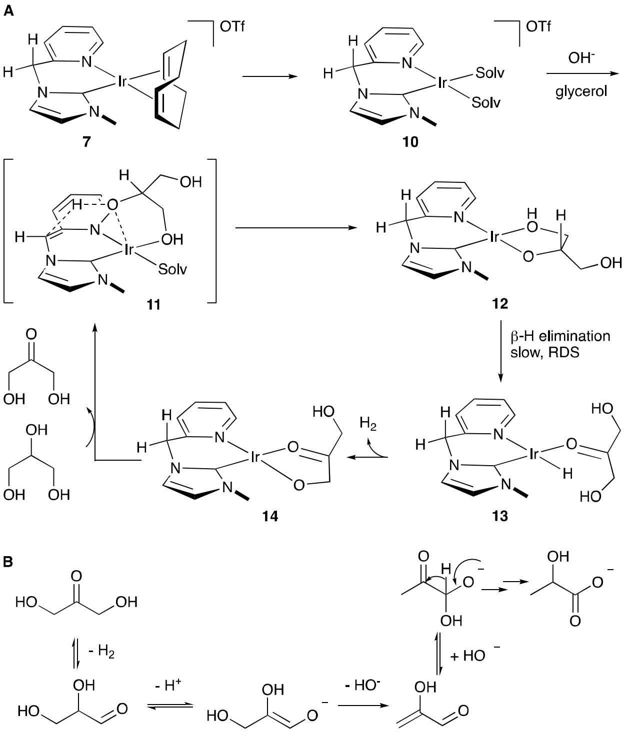

Scheme 3. Proposed stepwise glycerol dehydrogenation by **7** to yield lactate.

Direct observation of the catalytic cycle was impeded by speciation of the iridium complex under catalytic conditions: we believe the catalyst rests as a glycerol chelate, which must necessarily have many geometrical isomers. However, indirect interrogation provided enough information for a working understanding of the reaction mechanism (Scheme 3A). NMR evidence first establishes that iridium **7** is initiated by loss of COD, initially as cyclooctene. Kinetic studies show that the first step in the catalysis is most likely a deprotonation of the ligand on the iridium species, which allows an interaction with glycerol, apparently in a dual-center activation shown as **11**. We propose that a β-hydride elimination of an iridium alkoxide is the rate-determining step, based on first order kinetic dependence on alcohol and a negligible O—H kinetic isotope effect (1.1(1)) that excludes a bifunctional C—H/O—H dual activation. At the reaction operating temperature, there is little discrimination between the secondary alcohol and primary alcohol in glycerol, respectively yielding a ketone or an aldehyde product. These two products interconvert rapidly under the conditions; we perceive that this is unselective, because we find that 1- and 2-propanol react with similar rates. Once formed, glyceraldehyde is quickly converted to lactate in the presence of base (Scheme 3B), far too quickly for glyceraldehyde to be observed. Whereas the chirality of the product is established by a hydride migration taking place in the absence of the catalyst and at a barrier far lower than the oxidation, we perceive that this reaction is not a good target for asymmetric catalysis. Moreover, chirality of (L)-lactic acid that is formed by fermentation is typically destroyed when it is thermally oligomerized in poly(lactic acid) synthesis. We therefore see little motivation to control this chirality.

Iridium complex **7** is a general catalyst for dehydrogenation of alcohol. Complex **7** dehydrogenates methanol to carbonates in an alkaline medium. Detailed exploration of alcohol dehydrogenation reactivity of **1** and **7** is provided in section 2.4.

2.3 Hydrogen transfer from glyceride to fatty esters

Direct conversion of crude glycerol to lactate is an appealing complement to conversion of vegetable triglycerides to biodiesel, however it has an intrinsic inefficiency in that one equivalent of hydrogen is released from the reaction and would most probably be discarded as waste by many practitioners. Simultaneously, most vegetable oils are highly unsaturated, which is problematic if these are to be burned in a diesel engine. This situation presages the question of whether hydrogen from glycerol conversion can be used to upgrade biodiesel in the same reactor. Striking such a balance of glycerol oxidation and fatty acid reduction requires a delicate balance of catalyst stability, hydricity, and redox kinetics that, if achieved, could give rise to a very high utility tandem hydrogen transfer process.

The U.S. is the world's largest biodiesel manufacturer, and more than 80% of U.S. biodiesel originates from transesterification of soybean or corn oil. Both of these oils bear more than 50% polyunsaturated fatty acids, mostly the doubly-unsaturated linoleic acid (18:2) and a small portion of the triply-unsaturated linolenic acid (18:3).[110] In each case, the olefins of the fatty acids are segregated by single methylene groups whose C—H bonds are doubly activated for homolytic cleavage by the proximity of the two flanking alkenyl systems. Without hydrogenation of these olefins, biodiesels made from these polyunsaturated oils are unstable to oxidation of the activated methylene, leading to problems such as gum formation, oil filter clogging, tart deposition in engine, and slow ignition. Such problems reduce the overall value of biodiesel.[111,112] Hydrogenation conditions such as palladium/H_2 involve cost and safety issues (from handling compressed H_2)[113] and give fully saturated fatty acid chains. These are disadvantages; particularly, the latter causes a new problem of high melting point and propensity for precipitation in the fuel system.[114,115] Transfer hydrogenation is an appealing solution to these problems, and glycerol itself is an outstanding candidate to be the hydrogen donor. This concept is sketched in scheme 4. As with most catalytic processes, selectivity plays an important role on the outcome of this proposed reaction: the biodiesel upgrading should stop at one degree of unsaturation, which sets up a challenge of finding a selective *poly*-ene reduction catalyst.

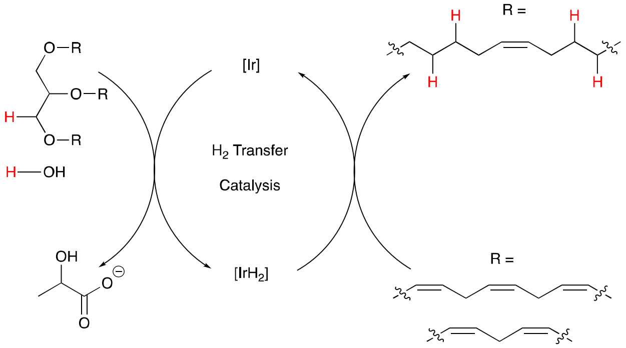

Scheme 4. Hydrogen transfer from glycerol to polyunsaturated fatty acids.

Iridium complex **7** achieves the right balance of hydrogen transfer rates and stability needed to execute the proposed tandem catalysis in scheme 4 with high selectivity, leaving exactly one degree of unsaturation in the products of polyunsaturation fatty acid. Glycerol is dehydrogenated selectively to lactate, and all polyunsaturation is reduced to monounsaturation with no other product observed in NMR. While this can be done on many triglyceride feedstocks, the reaction optimization using corn oil is summarized in table 1. It is important to note that there is not enough hydrogen imbedded in the glycerol of the triglycerides to achieve mass balance. Scheme 4 highlights the issue: only one equivalent of H_2 is available in the glycerol while more than one are needed to effect full conversion of polyunsaturation in all three of the glycerol's fatty acids. In a typical corn oil sample, the triglyceride has about 4.5 degrees of unsaturation per glycerol, and the product blend will have about 2.5 degrees per glycerol: a further reducing equivalent must be provided.

Table 1. Hydrogenation of polyunsaturation in corn oil to monounsaturation.[a]

Entry	Reductant (equiv.)			Degree of hydrogenation
	MeOH	Glycerol	H_2	
1[b]	25	0	0	100%
2[c]	0	25	0	99%
3[d]	0	25	0	90%
4[e]	0	25	0	25%
5	0	0	1 atm	62% (18% [f])

[a] Reaction condition: 0.5 mL corn oil, 0.3 mol% Ir complex, 5 eq. NaOH, 120 °C, 1 day in a sealed flask. Degree of hydrogenation refers to the portion of 2nd and 3rd olefins that are reduced to oleate. Oleate and saturated fatty esters are not derivatized in this reaction. [b] 1.0 equiv. lactate also formed. [c] 10 equiv. NaOH was used to obtain 11 equiv. of lactate. [d] 25 equiv. NaOH was used to obtain 19 equiv. of lactate. [e] Operated in a flask connected to a eudiometer. [f] No base was added.

Several features of the tandem catalysis make the process quite appealing. First, the choice of the external reductant is flexible. Both methanol and glycerol are abundant materials in the biodiesel industry, and each of them works well. Second, the catalytic system is water and air tolerant: the catalysis shows no change in kinetic behavior when prepared in air with 200 equiv. added water. Thirdly, while the price of iridium is prohibitive in most fuel cycle applications, our catalyst can be recovered by extraction and reused in a subsequent catalytic run. This iridium recovery method reduces the cost of metal below the value threshold of the synthetic lactate: to our calculations the value in the lactate by-product of upgrading is high enough to support the rental of the catalytic metal.

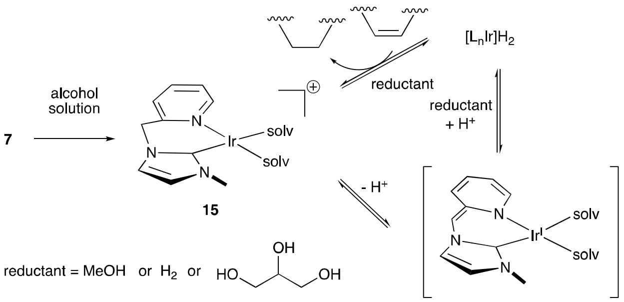

Scheme 5. Proposed base-accelerated pathway vs. base-free pathway.

While studying the mechanism of such catalytic systems can be frustrated by rapid speciation of the iridium, we were able to identify two possible pathways (Scheme 5). Precatalyst **7** is first initiated by reductive cleavage of COD to form **15**, a species observable in NMR, then the two possibilities diverge. In a simple system where H_2 is the reductant (e.g. Table 1, entry 5), both base-free and base-present conditions showed hydrogenation reactivity. However, when there is base, the reaction rate is accelerated several-fold. It is not obvious whether this reaction runs through liberation of intermediate H_2 gas, which is later re-activated or whether a catalytic metal hydride directly deposits hydride on its target olefin without reforming the H—H bond. A comparison between entries 4 and 5 in table 1 provides insight: it appears that both mechanisms are working at competitive rates in these respective conditions. The conversion appears slightly faster in direct hydrogen transfer, which is apparently the major path in entry 4, but H_2 formation and re-activation must be possible in order for entry 5 to function at the observed yield.

Although full hydrogenation of fatty acids results in lower value biodiesel product, these saturated fatty acids have value as fine chemicals. We find that iridium complex **7** can reduce polyunsaturation at a catalyst loading of 30 ppm but will only reduce monounsaturation at high (6 mol%) catalyst loading. To mitigate the cost of iridium, a second hydrogenation catalyst (**16**) was introduced. Although not a good dehydrogenation catalyst for glycerol, **16** proved to be a useful hydrogenation catalyst, enabling up to 90% hydrogenation of all unsaturation (Table 2). Although air sensitivity of **16** can be an issue in some contexts, we did not find this problematic in this reaction.

Table 2. Full hydrogenation of vegetable oil fatty acids.[a]

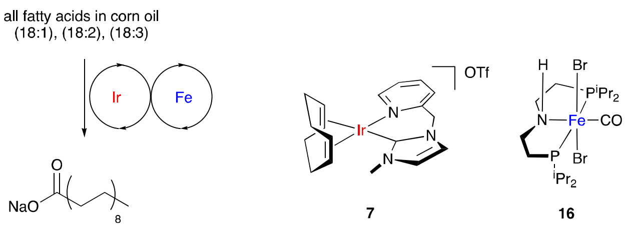

Entry	Ir precursor	Fe precursor	full hydrogenation
1	**7** (6 mol%)	NA	95%
2	NA	**16** (0.3 mol%)	7%
3	**7** (0.3 mol%)	**16** (0.3 mol%)	21%
4	**7** (0.3 mol%)	**16** (0.6 mol%)	34%
5	**7** (0.3 mol%)	**16** (3.0 mol%)	90%

[a] Reaction condition: 0.5 mL corn oil, 5 eq. NaOH, 25 eq. MeOH, 120 °C, 1 day in a sealed flask.

2.4 Application to fine chemicals: carboxylate synthesis

Discovery of structurally novel, prolific, and selective catalysts for fuel cycle applications opens the door to apply these same systems to problems of fine chemical synthesis. In these applications, the high value of the products formed enables more room to design molecular complexity, and thus cost, into a catalytic architecture. While it is unlikely that any complex, precious metal catalyst will be value-positive in a fuel application, linking such reactions to a fine chemical (as in the lactate presented in the prior example), or a complex molecule adds justification for the use of synthetic ligands and high-value metals. Thus, we test our hydrogen transfer catalysts in important reactions in fine chemicals and complex molecule synthesis applications.

We find that our iridium(I) complexes have useful activity in acceptorless dehydrogenation of primary alcohols to carboxylates in the presence of KOH (Scheme 7).[116] This is valuable, because while we have known since 1841 that heating primary alcohols with metal hydroxides can result in carboxylate formation,[117] most complex molecules are not tolerant of the requisite 350 °C reaction temperature for that transformation. Rather, we frequently employ high valent chromium, sulfur, iodine, or manganese reagents to effect such transformations, thus generating costly stoichiometric waste streams.

It is only in the last decade that a number of homogeneous catalytic methods have appeared for the conversion of primary alcohols to carboxylic acids. Rhodium based catalytic systems require hydrogen acceptors,[118–120] while ruthenium complexes **23** – **25** enable acceptorless dehydrogenation.[121–123] Recently, Fujita's group reported the first iridium based catalytic system that converts simple benzyl alcohols directly to benzoic acids in water without any base and hydrogen acceptor (Scheme 6).[124] Still, because each of these systems has restrictive limits on substrate scope, we set about to determine the utility of our catalysts in this transformation.

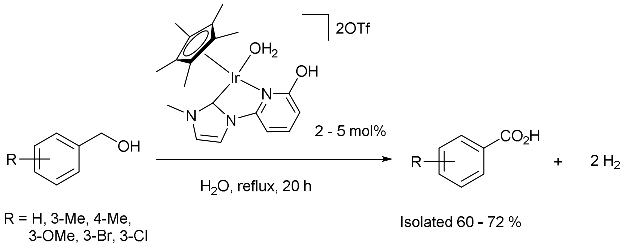

Scheme 6. Catalytic alcohol dehydrogenation by Fujita.

We find that both complexes **1** and **7** are excellent pre-catalysts for selective conversion of primary alcohols to carboxylates. The interchangeability of **1** and **7** in this reaction was not expected, since they have mutually exclusive activities in formic acid and glycerol dehydrogenation, respectively. We demonstrated a wide substrate scope and a unique functional group tolerance of our catalytic method. For example, secondary amines, thioethers, pyridines, and quinolines remain intact under the reaction conditions; this type of functional group tolerance was not previously observed for this reaction.

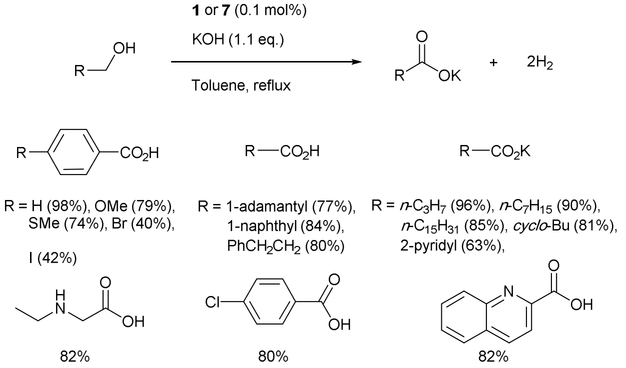

Scheme 7. Catalytic alcohol dehydrogenation with **1** and **7**.

Further, there had not yet been an exhaustive study on the mechanism of catalytic primary alcohol dehydrogenation, so we endeavored to get insight into the activation of pre-catalysts **1** and **7** in the catalytic mechanism. Traditionally, phosphines and NHC carbenes are thought to have similar coordinative properties.[125] Our observations highlight different behavior of **1** and **7** in catalyst initiation (Scheme 8). Thus, **1** reacts with an alcohol and KOH to give stable iridium(III) hydride complex **2**, whereas **7** forms reactive iridium(I) alkoxide **19** under the same conditions. We believe that formation of **2** proceeds through an iridium alkoxide analogous to **17**, which undergoes β-hydride elimination from the alkoxide ligand and isomerisation of η^2,η^2-COD to η^1,η^3-C_8H_{12}. This transformation was observed previously in the synthesis of **26**.[126]

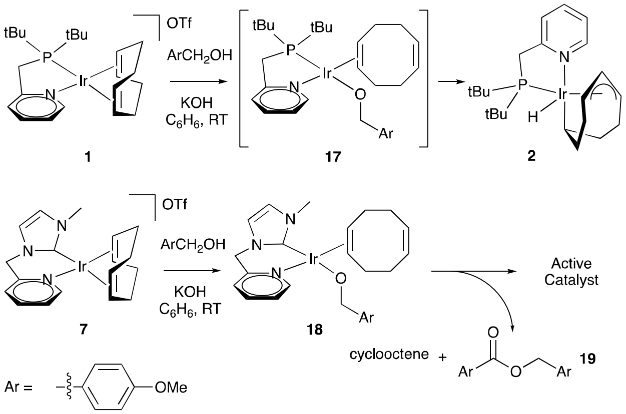

Scheme 8. Reactions of **1** and **7** with alcohols and KOH at 25 °C.

When **1** and **7** are subjected to the catalytic reaction conditions (alcohol, KOH, toluene, reflux), different organometallic species are observed. Only one iridium-containing intermediate is detected in the case of **7**: alkoxide **17** formed rapidly, then converts to the active catalyst. On the contrary, **1** converts to a mixture of dinuclear iridium hydride complexes **20** – **22** after a few turnovers (Scheme 9). We find that **20** – **22** are the catalyst resting states, and that they interconvert during catalysis. While we suspect that analogous species are involved in the initiation of **7** as in the initiation of **1**, we propose that the carbene-supported iridium hydrides are made electron rich by the combination of hydride and carbon ligands and are thus too reactive to observe cleanly.

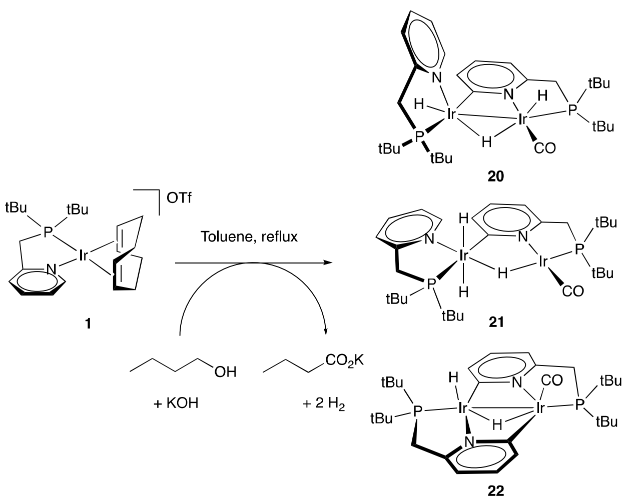

Scheme 9. Reaction of **1** with 1-butanol and KOH at 111 °C.

Several structural features of complexes **20** – **22** deserve discussion. The first is the CO ligand that emerges in catalyst activation. Iridium complexes enable decarbonylation of aldehydes,[127–130] which we find to be the origin of our CO ligand. Interestingly, we do not observe decarbonylation of glyceraldehyde with the same catalyst. Tandem iridium catalyzed dehydrogenative decarbonylation of alcohols is known,[131,132] but we do not observe this potential side-reaction, probably due to the presence of KOH, which promotes conversion of the aldehyde intermediate to the corresponding hemiacetal. Another structural feature is the catalyst's *ortho*-metalated pyridyl moieties. *ortho*-Metalation of pyridines by iridium via C–H activation is also known.[133–135] We like to think of the coordination environment of the carbonylated iridium atom as a mimic of an iridium bound into a PNP pincer complex like **28**.[136] We think about the non-carbonylated iridium center in **20** as an analog of the second phosphorus atom in **28**. Further stabilization of the diiridium core in **20** is facilitated by *ortho*-metalation of the pyridyl fragment at high temperature, yet the reversibility of this cyclometallation leaves our Ir—Ir bond labile to open as needed for catalysis.

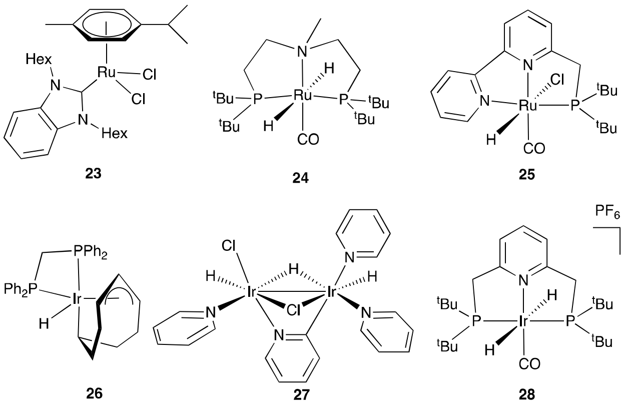

Figure 3. Structures of Iridium Complexes **23**-**28**.

The proposed mechanism of pre-catalyst **1** activation is shown in scheme 10. The process begins with a nucleophilic attack of an alkoxide on the iridium atom producing alkoxo complex **17** followed by β-hydride elimination and cyclooctadiene isomerization to give **2**. Complex **2** proceeds at elevated temperature to give dinuclear species **20** – **23**, which are in equilibrium. It is likely that **23** provides access to the catalytic cycle via reaction with an aldehyde. We do not know the structures of iridium species participating in the catalytic cycle, however we propose that the cycle involves β-hydride elimination from a diiridium alkoxo complex followed by reductive elimination of dihydrogen.

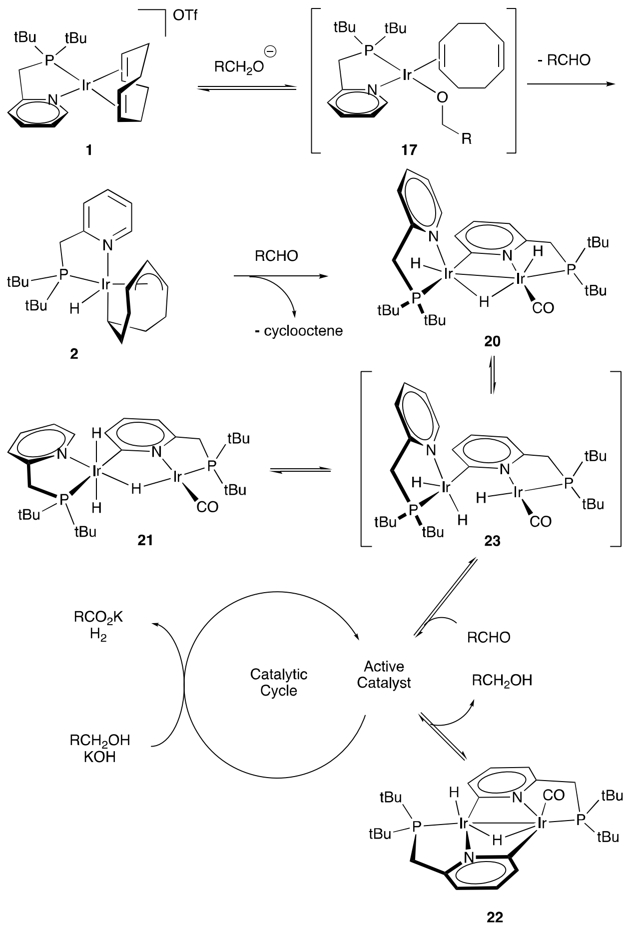

Scheme 10. Mechanism of pre-catalyst **1** activation.

2.5 The difference between iridium and ruthenium: an application in amination

While we achieved our best results in the reactions above using iridium complexes, we constantly apply our ligand design ideas to other metals in search of superior or orthogonal reactivity. For example, iridium and iron catalysts have complementary reactivity in biodiesel upgrading. We have historically had great success using ruthenium complexes in dehydrogenation reactions,[38,137–140] but we found that ruthenium complexes of our pyridyl phosphine ligand did not give useful reactivity with glycerol or formic acid, affording poor stability and uncontrolled, unselective reactions. By remarkable contrast—and quite unlike iridium chelates of the same P—N ligand—analogous ruthenium complexes do not convert alcohols to the corresponding carboxylate complexes, but rather participate in amination by hydrogen borrowing.[141]

Table 3 illustrates some striking observations from the scope of hydrogen borrowing amination realized with ruthenium P—N chelate **29**. We were surprised to learn that the indoles such as **30** and **32** did not poison the catalyst, but rather were well tolerated. We were even more surprised to find that delicate, reduction-sensitive groups like aryl iodide **31** were successfully converted to product with little over-reduction of the aryl halide group (entry 2). We take this as evidence that the intermediate ruthenium hydride species is not long lived (we never observed it) and reacts specifically with carbonyl and imine groups. Most amazing among the several examples we found were those presented with both an alkyl amine and an aniline. We were able to achieve selective alkylation of the alkyl amine in the presence of these anilines (entries 3, 4)! This is unprecedented and very useful reactivity to add to the literature of hydrogen borrowing amination.

We believe that the reason for this unanticipated selectivity is that the redox steps are too fast to allow imine formation to equilibrate. For example, introduction of deuterium labels into our starting alcohol enables us to observe the scrambling of those labels between the starting alcohol and amine faster than any coupling can be observed. We propose, therefore, that since the redox is fast, we can realize kinetic selectivity for imine formation and execute reactions that should not be possible when delicate functional groups are allowed to compete thermodynamically for imine formation with the intermediate aldehyde. This scenario, a straightforward modification of the traditional hydrogen borrowing mechanism, is outlined in scheme 11.

Table 3. Unanticipated selectivity in amination.

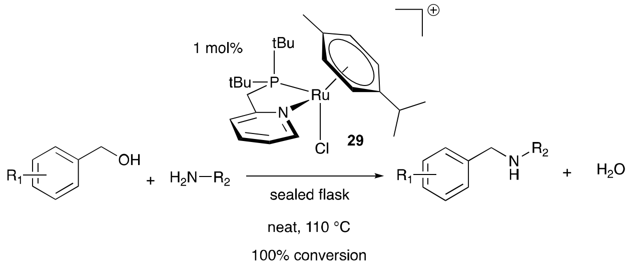

Entry	Alkylated amine	Time (hr)	Isolated yield (%)
1	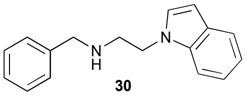 **30**	20	74
2	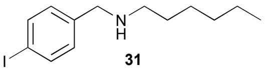 **31**	20	65
3	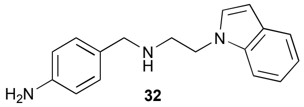 **32**	12	57
4	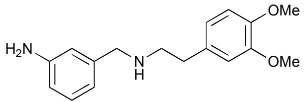 **33**	3	72

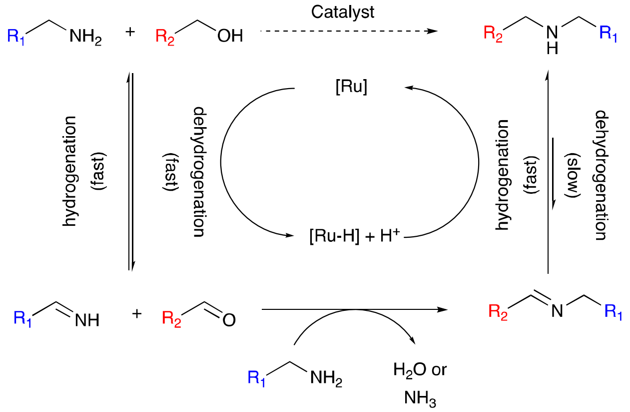

Scheme 11. Amination by hydrogen borrowing: fast redox enables unanticipated chemoselectivity.

3. A Unifying Hypothesis

Returning to our iridium story, we looked back on the surprisingly differentiated reactivities that we realized for apparently analogous species **1** and **7** and found in our mechanistic work some general guidelines that helped us to understand how and why catalyst initiation governs reactivity as these two very similar precursors enable mutually exclusive reactivity in some cases and nearly identical reactivity in others. These ideas are summarized in scheme 12.

In all cases, we anticipate that catalysis initiates with reductive cleavage of the 1,5-COD ligand. This proceeds by coordination of the metal to a hydride donor (alcohol, formate, H_2) and formation of a transient iridium hydride. This hydride then appears to insert into the COD ligand, which then isomerizes to from intermediate **2'**. From here a proton donor (e.g. RO—H) adds to the complex to form the C8 by-product, cyclooctene. Mechanistic pathways differentiate from this intermediate coordination complex, **17'**.

When L = P^tBu_2, **17'** goes on to form centrosymmetric dimer **4**. In the presence of a carboxylate substrate, this irreversibly converts to the C2-symmetric formic acid catalyst, **5**. In the presence of a CO donor, such as an aldehyde, one equivalent of **17'** carbonylates, which appears to touch off a dimerization sequence that leads to the equilibrium of **20**-**22**: these are the carboxylate synthesis catalyst. In the absence of a carboxylate or CO precursor, intermediate **17'** appears to engage in ligand substitution to give an iridium(I) chelate species. In the presence of glycerol, this appears to be a system of isomeric glycerol chelates, which we propose to be resting states of our glycerol to lactic acid catalyst.

4. Conclusions

The dehydrogenation of small molecules both for production of H_2 and formation of value-added products continues to be an important endeavor in catalysis. Large scale use of these transformations has the potential to mitigate many environmental and economic problems. While empirical screening approaches to catalyst discovery are meritorious, and can be effective in many cases, each of the reactions presented here is an example of hypothesis- and mechanism-directed catalyst development: without understanding how these systems initiate, compete for substrate, and eventually die, we would have been unable to realize the selectivity and longevity needed to make them useful and broadly applicable. We hope that these stories of directed discovery will inspire others, as they inspire us, to develop deep, relevant mechanistic understanding to motivate future research.

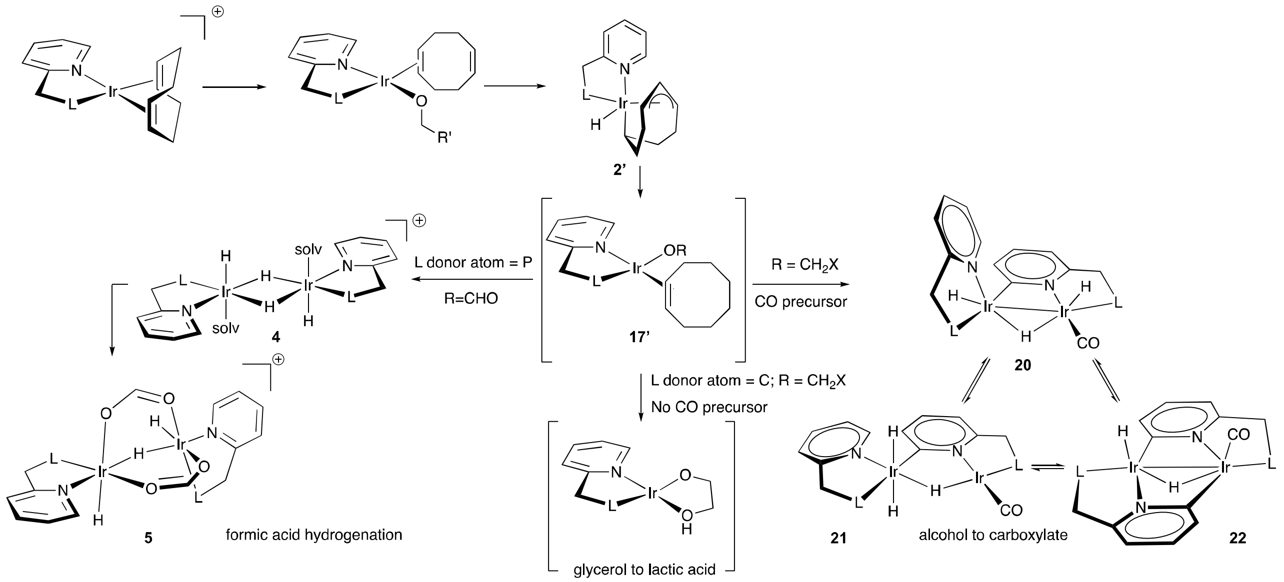

Scheme 12. A unifying proposal.

Conflicts of interest

Authors Lu and Williams have formed a company, Catapower, Inc., to pursue commercialization of the process outlined in scheme 3. We have collected no royalties for profits from this work to date.

Acknowledgements

This work is sponsored by the NSF (CHE-1566167), and the Hydrocarbon Research Foundation. We thank the NSF (DBI-0821671, CHE-0840366, CHE-1048807) and the NIH (S10 RR25432) for analytical instrumentation. We thank Prof. Ralf Haiges for help with X-ray crystallography. Fellowship assistance from USC Dornsife College (ID, VC), USC Provost and Rose Hills foundations (PJL) and the Jerome Sonosky fellowship provided through the Wrigley Institute for Environmental Studies (ID, VC) is gratefully acknowledged.

Notes and references

1 A. Kumar, T. M. Bhatti and A. S. Goldman, Dehydrogenation of Alkanes and Aliphatic Groups by Pincer-Ligated Metal Complexes, *Chem. Rev.*, 2017, **117**, 12357–12384.
2 R. H. Crabtree, Homogeneous transition metal catalysis of acceptorless dehydrogenative alcohol oxidation: applications in hydrogen storage and to heterocycle synthesis, *Chem. Rev.*, 2017, **117**, 9228–9246.
3 K. I. Goldberg and A. S. Goldman, Homogeneous transition metal catalysis of acceptorless dehydrogenative alcohol oxidation: applications in hydrogen storage and to heterocycle synthesis, *Acc. Chem. Res.*, 2017, **50**, 620–626.
4 R. M. Bullock and G. M. Chambers, Frustration across the periodic table: heterolytic cleavage of dihydrogen by metal complexes, *Philos. Trans. R. Soc. A Math. Eng. Sci.*, 2017, **375**, 20170002.
5 W. H. Bernskoetter and N. Hazari, Reversible Hydrogenation of Carbon Dioxide to Formic Acid and Methanol: Lewis Acid Enhancement of Base Metal Catalysts, *Acc. Chem. Res.*, 2017, **50**, 1049–1058.
6 S. Fukuzumi, Y. M. Lee and W. Nam, Thermal and photocatalytic production of hydrogen with earth-abundant metal complexes, *Coord. Chem. Rev.*, 2018, **355**, 54–73.
7 K. Sordakis, C. Tang, L. K. Vogt, H. Junge, P. J. Dyson, M. Beller and G. Laurenczy, Homogeneous catalysis for sustainable hydrogen storage in formic acid and alcohols, *Chem. Rev.*, 2018, **118**, 372–433.
8 G. Chelucci, Metal-catalyzed dehydrogenative synthesis of pyrroles and indoles from alcohols, *Coord. Chem. Rev.*, 2017, **331**, 37–53.
9 M. Andérez-Fernández, L. K. Vogt, S. Fischer, W. Zhou, H. Jiao, M. Garbe, S. Elangovan, K. Junge, H. Junge, R. Ludwig and M. Beller, A Stable Manganese Pincer Catalyst for the Selective Dehydrogenation of Methanol, *Angew. Chemie - Int. Ed.*, 2017, **56**, 559–562.
10 S. Aroua, T. K. Todorova, V. Mougel, P. Hommes, H. U. Reissig and M. Fontecave, New Cobalt-Bisterpyridyl Catalysts for Hydrogen Evolution Reaction, *ChemCatChem*, 2017, **9**, 2099–2105.
11 S. Y. De Boer, T. J. Korstanje, S. R. La Rooij, R. Kox, J. N. H. Reek and J. I. Van Der Vlugt, Ruthenium PNN(O) Complexes: Cooperative Reactivity and Application as Catalysts for Acceptorless Dehydrogenative Coupling Reactions, *Organometallics*, 2017, **36**, 1541–1549.
12 K. I. Fujita, R. Tamura, Y. Tanaka, M. Yoshida, M. Onoda and R. Yamaguchi, Dehydrogenative oxidation of alcohols in aqueous media catalyzed by a water-soluble dicationic iridium complex bearing a functional N-heterocyclic carbene ligand without using base, *ACS Catal.*, 2017, **7**, 7226–7230.
13 K. I. Fujita, T. Wada and T. Shiraishi, Reversible Interconversion between 2,5-Dimethylpyrazine and 2,5-Dimethylpiperazine by Iridium-Catalyzed Hydrogenation/Dehydrogenation for Efficient Hydrogen Storage, *Angew. Chemie - Int. Ed.*, 2017, **56**, 10886–10889.
14 G. González Miera, E. Martínez-Castro and B. Martín-Matute, Acceptorless Alcohol Dehydrogenation: OH vs NH Effect in Bifunctional NHC-Ir(III) Complexes, *Organometallics*, 2018, **37**, 636–644.
15 C. Guan, D.-D. Zhang, Y. Pan, M. Iguchi, M. J. Ajitha, J. Hu, H. Li, C. Yao, M.-H. Huang, S. Min, J. Zheng, Y. Himeda, H. Kawanami and K.-W. Huang, Dehydrogenation of Formic Acid Catalyzed by a Ruthenium Complex with an *N,N*′-Diimine Ligand, *Inorg. Chem.*, 2017, **56**, 438–445.
16 K. H. He, F. F. Tan, C. Z. Zhou, G. J. Zhou, X. L. Yang and Y. Li, Acceptorless Dehydrogenation of N-Heterocycles by Merging Visible-Light Photoredox Catalysis and Cobalt Catalysis, *Angew. Chemie - Int. Ed.*, 2017, **56**, 3080–3084.
17 W. C. Henke, D. Lionetti, W. N. G. Moore, J. A. Hopkins, V. W. Day and J. D. Blakemore, Ligand Substituents Govern the Efficiency and Mechanistic Path of Hydrogen Production with [Cp*Rh] Catalysts, *ChemSusChem*, 2017, **10**, 4589–4598.
18 G. Jaiswal, V. G. Landge, D. Jagadeesan and E. Balaraman, Iron-based nanocatalyst for the acceptorless dehydrogenation reactions, *Nat. Commun.*, 2017, 2147.
19 E. H. Kwan, H. Ogawa and M. Yamashita, A Highly Active PBP–Iridium Catalyst for the Dehydrogenation of Dimethylamine–Borane: Catalytic Performance and Mechanism, *ChemCatChem*, 2017, **9**, 2457–2462.
20 A. Matsunami, S. Kuwata and Y. Kayaki, A Bifunctional Iridium Catalyst Modified for Persistent Hydrogen Generation from Formic Acid: Understanding Deactivation via Cyclometalation of a 1,2-Diphenylethylenediamine Motif, *ACS Catal.*, 2017, **7**, 4479–4484.
21 D. H. Nguyen, X. Trivelli, F. Capet, J. F. Paul, F. Dumeignil and R. M. Gauvin, Manganese Pincer Complexes for the Base-Free, Acceptorless Dehydrogenative Coupling of Alcohols to Esters: Development, Scope, and Understanding, *ACS Catal.*, 2017, **7**, 2022–2032.

22 A. Rana, B. Mondal, P. Sen, S. Dey and A. Dey, Activating Fe(I) Porphyrins for the Hydrogen Evolution Reaction Using Second-Sphere Proton Transfer Residues, *Inorg. Chem.*, 2017, **56**, 1783–1793.

23 S. J. C. Robinson and D. M. Heinekey, Hydride & dihydrogen complexes of earth abundant metals: structure, reactivity, and applications to catalysis, *Chem. Commun.*, 2017, **53**, 669–676.

24 K. Sordakis, A. Tsurusaki, M. Iguchi, H. Kawanami, Y. Himeda and G. Laurenczy, Aqueous phase homogeneous formic acid disproportionation into methanol, *Green Chem.*, 2017, **19**, 2371–2378.

25 M. Trincado, V. Sinha, R. E. Rodriguez-Lugo, B. Pribanic, B. De Bruin and H. Grützmacher, Homogeneously catalysed conversion of aqueous formaldehyde to H2 and carbonate, *Nat. Commun.*, 2017, 14990.

26 A. Tsurusaki, K. Murata, N. Onishi, K. Sordakis, G. Laurenczy and Y. Himeda, Investigation of Hydrogenation of Formic Acid to Methanol using H $_2$ or Formic Acid as a Hydrogen Source, *ACS Catal.*, 2017, **7**, 1123–1131.

27 C. Wang and J. Xiao, Iridacycles for hydrogenation and dehydrogenation reactions, *Chem. Commun.*, 2017, **53**, 3399–3411.

28 M. Wilklow-Marnell, B. Li, T. Zhou, K. Krogh-Jespersen, W. W. Brennessel, T. J. Emge, A. S. Goldman and W. D. Jones, Catalytic Dehydrogenative C-C Coupling by a Pincer-Ligated Iridium Complex, *J. Am. Chem. Soc.*, 2017, **139**, 8977–8989.

29 F. Kallmeier and R. Kempe, Manganese Complexes for (De) Hydrogenation Catalysis: A Comparison to Cobalt and Iron Catalysts, *Angew. Chemie - Int. Ed.*, 2018, **57**, 46–60.

30 Y. Nakahara, T. Toda, A. Matsunami, Y. Kayaki and S. Kuwata, Protic NNN and NCN Pincer-Type Ruthenium Complexes Featuring (Trifluoromethyl)pyrazole Arms: Synthesis and Application to Catalytic Hydrogen Evolution from Formic Acid, *Chem. - An Asian J.*, 2018, **13**, 73–80.

31 H. Ando, S. Kusumoto, W. Wu and K. Nozaki, Cp∗Ir-Catalyzed Acceptorless Dehydrogenation of Carbon-Carbon Single Bonds, *Organometallics*, 2017, **36**, 2317–2322.

32 S. Cohen, V. Borin, I. Schapiro, S. Musa, S. De-Botton, N. V. Belkova and D. Gelman, Ir(III)-PC(sp ^{3})P Bifunctional Catalysts for Production of H $_2$ by Dehydrogenation of Formic Acid: Experimental and Theoretical Study, *ACS Catal.*, 2017, **7**, 8139–8146.

33 Z. Dai, Q. Luo, H. Jiang, Q. Luo, H. Li, J. Zhang and T. Peng, Ni(<scp>ii</scp>)–N′NN′ pincer complexes catalyzed dehydrogenation of primary alcohols to carboxylic acids and H $_2$ accompanied by alcohol etherification, *Catal. Sci. Technol.*, 2017, **7**, 2506–2511.

34 G. W. Crabtree, M. S. Dresselhaus and M. V. Buchanan, The Hydrogen Economy, *Phys. Today*, 2004, **57**, 39–44.

35 D. P. Gregory, *The Hydrogen Economy*, 1973, vol. 228.

36 U. Bossel and B. Eliasson, *The Future of the Hydrogen Economy*, 2005.

37 R. Dahlberg, Replacement of fossil fuels by hydrogen, *Int. J. Hydrogen Energy*, 1982, **7**, 121–142.

38 X. Zhang, L. Kam, R. Trerise and T. J. Williams, Ruthenium-Catalyzed Ammonia Borane Dehydrogenation: Mechanism and Utility, *Acc. Chem. Res.*, 2017, 86–95.

39 T. Abbasi and S. A. Abbasi, 'Renewable'hydrogen: prospects and challenges, *Renew. Sustain. Energy Rev.*, 2011, **15**, 3034–3040.

40 X. Zhang, Z. Lu, L. K. Foellmer and T. J. Williams, Nitrogen-Based Ligands Accelerate Ammonia Borane Dehydrogenation with the Shvo Catalyst, *Organometallics*, 2015, **34**, 3732–3738.

41 O. Z. Sharaf and M. F. Orhan, An overview of fuel cell technology: Fundamentals and applications, *Renew. Sustain. Energy Rev.*, 2014, **32**, 810–853.

42 S. Enthaler, Carbon Dioxide-The Hydrogen-Storage Material of the Future?, *ChemSusChem*, 2008, **1**, 801–804.

43 R. Tanaka, M. Yamashita and K. Nozaki, Catalytic Hydrogenation of Carbon Dioxide Using Ir(III)-Pincer Complexes, *J. Am. Chem. Soc.*, 2009, **131**, 14168–14169.

44 A. Boddien, B. Loges, H. Junge and M. Beller, Hydrogen Generation at Ambient Conditions: Application in Fuel Cells, *ChemSusChem*, 2008, **1**, 751–758.

45 B. Loges, A. Boddien, H. Junge and M. Beller, Controlled generation of hydrogen from formic acid amine adducts at room temperature and application in H2/O2 fuel cells, *Angew. Chemie - Int. Ed.*, 2008, **47**, 3962–3965.

46 Q.-L. Zhu, N. Tsumori and Q. Xu, Immobilizing Extremely Catalytically Active Palladium Nanoparticles to Carbon Nanospheres: A Weakly-Capping Growth Approach, *J. Am. Chem. Soc.*, 2015, **137**, 11743–11748.

47 Z. Zheng, T. Tachikawa and T. Majima, Plasmon-Enhanced Formic Acid Dehydrogenation Using Anisotropic Pd–Au Nanorods Studied at the Single-Particle Level, *J. Am. Chem. Soc.*, 2015, **137**, 948–957.

48 Y. Chen, Q.-L. Zhu, N. Tsumori and Q. Xu, Immobilizing Highly Catalytically Active Noble Metal Nanoparticles on Reduced Graphene Oxide: A Non-Noble Metal Sacrificial Approach, *J. Am. Chem. Soc.*, 2015, **137**, 106–109.

49 K. Jiang, K. Xu, S. Zou and W.-B. Cai, B-Doped Pd Catalyst: Boosting Room-Temperature Hydrogen Production from Formic Acid–Formate Solutions, *J. Am. Chem. Soc.*, 2014, **136**, 4861–4864.

50 Q.-L. Zhu, N. Tsumori and Q. Xu, Sodium hydroxide-assisted growth of uniform Pd nanoparticles on nanoporous carbon MSC-30 for efficient and complete dehydrogenation of formic acid under ambient conditions, *Chem. Sci.*, 2014, **5**, 195–199.

51 Z.-L. Wang, J.-M. Yan, Y. Ping, H.-L. Wang, W.-T. Zheng and Q. Jiang, An Efficient CoAuPd/C Catalyst for Hydrogen Generation from Formic Acid at Room Temperature, *Angew. Chemie Int. Ed.*, 2013, **52**, 4406–4409.

52 K. Mori, M. Dojo and H. Yamashita, Pd and Pd–Ag Nanoparticles within a Macroreticular Basic Resin: An Efficient Catalyst for Hydrogen Production from Formic Acid Decomposition, *ACS Catal.*, 2013, **3**, 1114–1119.

53 X. Gu, Z.-H. Lu, H.-L. Jiang, T. Akita and Q. Xu, Synergistic Catalysis of Metal–Organic Framework-Immobilized Au–Pd Nanoparticles in Dehydrogenation of Formic Acid for Chemical Hydrogen Storage, *J. Am. Chem. Soc.*, 2011, **133**, 11822–11825.

54 S. Zhang, Ö. Metin, D. Su and S. Sun, Monodisperse AgPd alloy nanoparticles and their superior catalysis for the dehydrogenation of formic acid, *Angew. Chemie - Int. Ed.*, 2013, **52**, 3681–3684.

55 Q.-Y. Bi, X.-L. Du, Y.-M. Liu, Y. Cao, H.-Y. He and K.-N. Fan, Efficient Subnanometric Gold-Catalyzed Hydrogen Generation via Formic Acid Decomposition under Ambient Conditions, *J. Am. Chem. Soc.*, 2012, **134**, 8926–8933.

56 K. Tedsree, T. Li, S. Jones, C. W. A. Chan, K. M. K. Yu, P. A. J. Bagot, E. A. Marquis, G. D. W. Smith and S. C. E. Tsang, Hydrogen production from formic acid decomposition at room temperature using a Ag–Pd core–shell nanocatalyst, *Nat. Nanotechnol.*, 2011, **6**, 302–307.

57 Y. Huang, X. Zhou, M. Yin, C. Liu and W. Xing, Novel PdAu@Au/C Core−Shell Catalyst: Superior Activity and Selectivity in Formic Acid Decomposition for Hydrogen Generation, *Chem. Mater.*, 2010, **22**, 5122–5128.

58 F. Bertini, I. Mellone, A. Ienco, M. Peruzzini and L. Gonsalvi, Iron(II) Complexes of the Linear *rac*- Tetraphos-1 Ligand as Efficient Homogeneous Catalysts for Sodium Bicarbonate Hydrogenation and Formic Acid Dehydrogenation, *ACS Catal.*, 2015, **5**, 1254–1265.

59 A. Thevenon, E. Frost-Pennington, G. Weijia, A. F. Dalebrook and G. Laurenczy, Formic Acid Dehydrogenation Catalysed by Tris(TPPTS) Ruthenium Species: Mechanism of the Initial “Fast” Cycle, *ChemCatChem*, 2014, **6**, 3146–3152.

60 S. Oldenhof, M. Lutz, B. de Bruin, J. Ivar van der Vlugt and J. N. H. Reek, Dehydrogenation of formic acid by Ir–bisMETAMORPhos complexes: experimental and computational insight into the role of a cooperative ligand, *Chem. Sci.*, 2015, **6**, 1027–1034.

61 T. W. Myers and L. A. Berben, Aluminium–ligand cooperation promotes selective dehydrogenation of formic acid to H_2 and CO_2, *Chem. Sci.*, 2014, **5**, 2771–2777.

62 P. Sponholz, D. Mellmann, H. Junge and M. Beller, Towards a Practical Setup for Hydrogen Production from Formic Acid, *ChemSusChem*, 2013, **6**, 1172–1176.

63 E. A. Bielinski, P. O. Lagaditis, Y. Zhang, B. Q. Mercado, C. Würtele, W. H. Bernskoetter, N. Hazari and S. Schneider, Lewis acid-assisted formic acid dehydrogenation using a pincer-supported iron catalyst, *J. Am. Chem. Soc.*, 2014, **136**, 10234–10237.

64 M. Czaun, A. Goeppert, J. Kothandaraman, R. B. May, R. Haiges, G. K. S. Prakash and G. A. Olah, Formic Acid As a Hydrogen Storage Medium: Ruthenium-Catalyzed Generation of Hydrogen from Formic Acid in Emulsions, *ACS Catal.*, 2014, **4**, 311–320.

65 Y. Manaka, W.-H. Wang, Y. Suna, H. Kambayashi, J. T. Muckerman, E. Fujita and Y. Himeda, Efficient H_2 generation from formic acid using azole complexes in water, *Catal. Sci. Technol.*, 2014, **4**, 34–37.

66 S. Oldenhof, B. de Bruin, M. Lutz, M. A. Siegler, F. W. Patureau, J. I. van der Vlugt and J. N. H. Reek, Base-Free Production of H_2 by Dehydrogenation of Formic Acid Using An Iridium-bisMETAMORPhos Complex, *Chem. - A Eur. J.*, 2013, **19**, 11507–11511.

67 I. Mellone, M. Peruzzini, L. Rosi, D. Mellmann, H. Junge, M. Beller and L. Gonsalvi, Formic acid dehydrogenation catalysed by ruthenium complexes bearing the tripodal ligands triphos and NP_3, *Dalt. Trans.*, 2013, **42**, 2495–2501.

68 J. F. Hull, Y. Himeda, W.-H. Wang, B. Hashiguchi, R. Periana, D. J. Szalda, J. T. Muckerman and E. Fujita, Reversible hydrogen storage using CO2 and a proton-switchable iridium catalyst in aqueous media under mild temperatures and pressures, *Nat. Chem.*, 2012, **4**, 383–388.

69 J. H. Barnard, C. Wang, N. G. Berry and J. Xiao, Long-range metal–ligand bifunctional catalysis: cyclometallated iridium catalysts for the mild and rapid dehydrogenation of formic acid, *Chem. Sci.*, 2013, **4**, 1234.

70 Y. Himeda, Highly efficient hydrogen evolution by decomposition of formic acid using an iridium catalyst with 4,4′-dihydroxy-2,2′-bipyridine, *Green Chem.*, 2009, **11**, 2018.

71 A. Boddien, D. Mellmann, F. Gartner, R. Jackstell, H. Junge, P. J. Dyson, G. Laurenczy, R. Ludwig and M. Beller, Efficient Dehydrogenation of Formic Acid Using an Iron Catalyst, *Science (80-.).*, 2011, **333**, 1733–1736.

72 C. Fellay, P. Dyson and G. Laurenczy, A Viable Hydrogen-Storage System Based On Selective Formic Acid Decomposition with a Ruthenium Catalyst, *Angew. Chemie Int. Ed.*, 2008, **47**, 3966–3968.

73 J. J. A. Celaje, Z. Lu, E. A. Kedzie, N. J. Terrile, J. N. Lo and T. J. Williams, A prolific catalyst for dehydrogenation of neat formic acid, *Nat. Commun.*, 2016, **7**, 11308.

74 Y. Gao, J. Kuncheria, R. J. Puddephatt and G. P. A. Yap, An efficient binuclear catalyst for decomposition of formic acid, *Chem. Commun.*, 1998, 2365–2366.

75 EPA, 2017 Renewable Fuel Standard Data.

76 K. Chung, S. M. Banik, A. G. De Crisci, D. M. Pearson, T. R. Blake, J. V. Olsson, A. J. Ingram, R. N. Zare and R. M. Waymouth, Chemoselective Pd-catalyzed oxidation of polyols: Synthetic scope and mechanistic studies, *J. Am. Chem. Soc.*, 2013, **135**, 7593–7602.

77 Y. Zhang, N. Zhang, Z.-R. Tang and Y.-J. Xu, Identification of Bi2WO6 as a highly selective visible-light photocatalyst toward oxidation of glycerol to dihydroxyacetone in water, *Chem. Sci.*, 2013, **4**, 1820.

78 G. L. Brett, Q. He, C. Hammond, P. J. Miedziak, N. Dimitratos, M. Sankar, A. A. Herzing, M. Conte, J. A. Lopez-Sanchez, C. J. Kiely, D. W. Knight, S. H. Taylor and G. J. Hutchings, Selective oxidation of glycerol by highly active bimetallic catalysts at ambient temperature under base-free conditions, *Angew. Chemie - Int. Ed.*, 2011, **50**, 10136–10139.

79 D. B. Lao, A. C. E. Owens, D. M. Heinekey and K. I. Goldberg, Partial deoxygenation of glycerol catalyzed by iridium pincer complexes, *ACS Catal.*, 2013, **3**, 2391–2396.

80 C. A. G. Quispe, C. J. R. Coronado and J. A. Carvalho, Glycerol: Production, consumption, prices, characterization and new trends in combustion, *Renew. Sustain. Energy Rev.*, 2013, **27**, 475–493.

81 M. Pagliaro, R. Ciriminna, H. Kimura, M. Rossi and C. Della Pina, *Angew. Chemie - Int. Ed.*, 2007, **46**, 4434–4440.

82 U.S. Department of Agriculture, Renewable Chemicals & Materials Opportunity Assessment.

83 N. Zargari, E. Jung, J. H. Lee and K. W. Jung, Carbon dioxide hydrogenation: Efficient catalysis by an NHC-amidate Pd(II) complex, *Tetrahedron Lett.*, 2017, **58**, 3330–3332.

84 K. Rohmann, J. Kothe, M. W. Haenel, U. Englert, M. Hölscher and W. Leitner, Hydrogenation of CO2to Formic Acid with a Highly Active Ruthenium Acriphos Complex in DMSO and DMSO/Water, *Angew. Chemie - Int. Ed.*, 2016, **55**, 8966–8969.

85 S. Moret, P. J. Dyson and G. Laurenczy, Direct synthesis of formic acid from carbon dioxide by hydrogenation in acidic media, *Nat Commun*, 2014, **5**, 4017.

86 C. A. Huff and M. S. Sanford, Catalytic CO2 hydrogenation to formate by a ruthenium pincer complex, *ACS Catal.*, 2013, **3**, 2412–2416.

87 G. A. Filonenko, R. Van Putten, E. N. Schulpen, E. J. M. Hensen and E. A. Pidko, Highly efficient reversible hydrogenation of carbon dioxide to formates using a ruthenium PNP-pincer catalyst, *ChemCatChem*, 2014, **6**, 1526–1530.

88 M. S. Jeletic, M. T. Mock, A. M. Appel and J. C. Linehan, A Cobalt-Based Catalyst for the Hydrogenation of CO 2under Ambient Conditions, *J. Am. Chem. Soc.*, 2013, **135**, 11533–11536.

89 S. F. Hsu, S. Rommel, P. Eversfield, K. Muller, E. Klemm, W. R. Thiel and B. Plietker, A rechargeable hydrogen battery based on Ru catalysis, *Angew. Chemie - Int. Ed.*, 2014, **53**, 7074–7078.

90 T. J. Schmeier, G. E. Dobereiner, R. H. Crabtree and N. Hazari, Secondary coordination sphere interactions facilitate the insertion step in an iridium(III) CO2 reduction catalyst, *J. Am. Chem. Soc.*, 2011, **133**, 9274–9277.

91 R. Langer, Y. Diskin-Posner, G. Leitus, L. J. W. Shimon, Y. Ben-David and D. Milstein, Low-pressure hydrogenation of carbon dioxide catalyzed by an iron pincer complex exhibiting noble metal activity, *Angew. Chemie - Int. Ed.*, 2011, **50**, 9948–9952.

92 C. Federsel, C. Ziebart, R. Jackstell, W. Baumann and M. Beller, Catalytic hydrogenation of carbon dioxide and bicarbonates with a well-defined cobalt dihydrogen complex, *Chem. - A Eur. J.*, 2012, **18**, 72–75.

93 C. Federsel, A. Boddien, R. Jackstell, R. Jennerjahn, P. J. Dyson, R. Scopelliti, G. Laurenczy and M. Beller, A well-defined iron catalyst for the reduction of bicarbonates and carbon dioxide to formates, alkyl formates, and formamides, *Angew. Chemie - Int. Ed.*, 2010, **49**, 9777–9780.

94 C. Federsel, R. Jackstell, A. Boddien, G. Laurenczy and M. Beller, Ruthenium-catalyzed hydrogenation of bicarbonate in water, *ChemSusChem*, 2010, **3**, 1048–1050.

95 J. J. A. Celaje, Z. Lu, E. A. Kedzie, N. J. Terrile, J. N. Lo and T. J. Williams, A prolific catalyst for dehydrogenation of neat formic acid, *Nat. Commun.*, 2016, **7**, 11308.

96 T. Zell and D. Milstein, Hydrogenation and Dehydrogenation Iron Pincer Catalysts Capable of Metal-Ligand Cooperation by Aromatization/Dearomatization, *Acc. Chem. Res.*, 2015, **48**, 1979–1994.

97 S. Gruber, M. Neuburger and A. Pfaltz, Characterization and reactivity studies of dinuclear iridium hydride complexes prepared from iridium catalysts with N,P and C,N ligands under hydrogenation conditions, *Organometallics*, 2013, **32**, 4702–4711.

98 D. J. Morris, G. J. Clarkson and M. Wills, Insights into hydrogen generation from formic acid using ruthenium complexes, *Organometallics*, 2009, **28**, 4133–4140.

99 R. Christoph, B. Schmidt, U. Steinberner, W. Dilla and R. Karinen, *Ullmann's Encycl. Ind. Chem.*, 2010, 16.

100 BP, BP Statistical Review of World Energy 2017, *BP Stat. Rev. World Energy*, 2017, 1–52.

101 L. S. Sharninghausen, J. Campos, M. G. Manas and R. H. Crabtree, Efficient selective and atom economic catalytic conversion of glycerol to lactic acid, *Nat. Commun.*, 2014, **5**, 5084.

102 D. Roy, B. Subramaniam and R. V. Chaudhari, Cu-based catalysts show low temperature activity for glycerol conversion to lactic acid, *ACS Catal.*, 2011, **1**, 548–551.

103 Y. Shen, S. Zhang, H. Li, Y. Ren and H. Liu, Efficient Synthesis of Lactic Acid by Aerobic Oxidation of Glycerol on Au-Pt/TiO2 Catalysts, *Chem. - A Eur. J.*, 2010, **16**, 7368–7371.

104 H. J. Cho, C.-C. Chang and W. Fan, Base free, one-pot synthesis of lactic acid from glycerol using a bifunctional Pt/Sn-MFI catalyst, *Green Chem.*, 2014, **16**, 3428–3433.

105 L. Chen, S. Ren and X. P. Ye, Lactic acid production from glycerol using CaO as solid base catalyst, *Fuel Process. Technol.*, 2014, **120**, 40–47.

106 M. Finn, J. A. Ridenour, J. Heltzel, C. Cahill and A. Voutchkova-Kostal, Next-Generation Water-Soluble Homogeneous Catalysts for Conversion of Glycerol to Lactic Acid, *Organometallics*, 2018, **37**, 1400-1409.

107 Z. Lu, I. Demianets, R. Hamze, N. J. Terrile and T. J. Williams, A Prolific Catalyst for Selective Conversion of Neat Glycerol to Lactic Acid, *ACS Catal.*, 2016, **6**, 2014–2017.

108 A. Wawrzetz, B. Peng, A. Hrabar, A. Jentys, A. A. Lemonidou and J. A. Lercher, Towards understanding the bifunctional hydrodeoxygenation and aqueous phase reforming of glycerol, *J. Catal.*, 2010, **269**, 411–420.

109 E. Farnetti, J. Kašpar and C. Crotti, A novel glycerol valorization route: chemoselective dehydrogenation catalyzed by iridium derivatives, *Green Chem.*, 2009, **11**, 704.

110 D. Pimentel and T. Patzek, Ethanol production using corn, switchgrass, and wood; Biodiesel production using soybean and sunflower, *Nat. Resour. Res.*, 2005, **14**, 65–76.

111 M. J. Ramos, C. M. Fernández, A. Casas, L. Rodríguez and Á. Pérez, Influence of fatty acid composition of raw materials on biodiesel properties, *Bioresour. Technol.*, 2009, **100**, 261–268.

112 H. M. Mahmudul, F. Y. Hagos, R. Mamat, A. A. Adam, W. F. W. Ishak and R. Alenezi, Production, characterization and performance of biodiesel as an alternative fuel in diesel engines – A review, *Renew. Sustain. Energy Rev.*, 2017, **72**,

497–509.
113 C. Thunyaratchatanon, A. Luengnaruemitchai, N. Chollacoop and Y. Yoshimura, Catalytic upgrading of soybean oil methyl esters by partial hydrogenation using Pd catalysts, *Fuel*, 2016, **163**, 8–16.
114 A. Demirbas, Biofuels sources, biofuel policy, biofuel economy and global biofuel projections, *Energy Convers. Manag.*, 2008, **49**, 2106–2116.
115 G. M. Chupka, L. Fouts, J. A. Lennon, T. L. Alleman, D. A. Daniels and R. L. McCormick, Saturated monoglyceride effects on low-temperature performance of biodiesel blends, *Fuel Process. Technol.*, 2014, **118**, 302–309.
116 V. Cherepakhin and T. J. Williams, Iridium Catalysts for Acceptorless Dehydrogenation of Alcohols to Carboxylic Acids: Scope and Mechanism., *ACS Catal.*, 2018, **8**, 3754–3763.
117 E. E. Reid, H. Worthington and L. A. W., The action of caustic alkali and of alkaline salts on alcohols, *J. Am. Chem. Soc.*, 1939, **61**, 99–101.
118 T. Zweifel, J. Naubron and H. Grützmacher, Catalyzed Dehydrogenative Coupling of Primary Alcohols with Water, Methanol, or Amines., *Chem. Int. Ed.*, 2009, **48**, 559–563.
119 M. Trincado, H. Grutzmacher, F. Vizza and C. Bianchini, Domino Rhodium/Palladium-Catalyzed Dehydrogenation Reactions of Alcohols to Acids by Hydrogen Transfer to Inactivated Alkenes., *Chem. Eur. J.*, 2010, **16**, 2751–2757.
120 S. Annen, T. Zweifel, F. Ricatto and H. Grutzmacher, Catalytic Aerobic Dehydrogenative Coupling of Primary Alcohols and Water to Acids Promoted by a Rhodium(I) Amido N-Heterocyclic Carbene Complex., *ChemCatChem*, 2010, **2**, 1286–1295.
121 J. Malineni, H. Keul and M. Möller, A Green and Sustainable Phosphine-Free NHC-Ruthenium Catalyst for Selective Oxidation of Alcohols to Carboxylic Acids in Water., *Dalt. Trans.*, 2015, **44**, 17409–17414.
122 J. Choi, L. E. Heim, M. Ahrens and M. H. G. Prechtl, ., Selective Conversion of Alcohols in Water to Carboxylic Acids by in situ Generated Ruthenium Trans Dihydrido Carbonyl PNP Complexes, *Dalt. Trans.*, 2014, **43**, 17248–17254.
123 E. Balaraman, E. Khaskin, G. Leitus and D. Milstein, Catalytic Transformation of Alcohols to Carboxylic Acid Salts and H2 Using Water as the Oxygen Atom Source, *Nat. Chem.*, 2013, **5**, 122–125.
124 K. Fujilta, R. Tamura, Y. Tanaka, M. Yoshida, M. Onoda and R. Yamaguchi, Dehydrogenative Oxidation of Alcohols in Aqueous Media Catalyzed by a Water-Soluble Dicationic Iridium Complex Bearing a Functional N-Heterocyclic Carbene Ligand without Using Base, *ACS Catal.*, 2017, **7**, 7226–7230.
125 W. A. Herrmann, M. Elison, J. Fischer, C. Köcher and G. R. J. Artus, N-heterocyclic carbenes[+]: Generation under mild conditions and formation of group 8-10 transition metal complexes relevant to catalysis, *Chem. - A Eur. J.*, 1996, **2**, 772–780.
126 M. A. Esteruelas, M. Olivan, L. A. Oro, M. Schulz, E. Sola and H. Werner, Synthesis, Molecular Structure and Reactivity of the Octahedral Iridium(III) Compound [IrH(η1,η3-C8H12)(dppm)] [dppm = bis(diphenylphosphino)methane], *Organometallics*, 1992, **11**, 3659–3664.
127 L. Vaska and J. W. DiLuzio, Carbonyl and hydrido-carbonyl complexes of iridium by reaction with alcohols. Hydrido complexes by reaction with acid, *J. Am. Chem. Soc.*, 1961, **83**, 2784–2785.
128 T. Iwai, T. Fujihara and Y. Tsuji, The Iridium-Catalyzed Decarbonylation of Aldehydes Under Mild Conditions, *Chem. Commun.*, 2008, 6215–6217.
129 A. E. Roa, V. Salazar, J. López-Serrano, E. Oñate, M. Paneque and M. L. Poveda, Decarbonylation of Aliphatic Aldehydes by a TpMe2Ir(III) Metallacyclopentadiene, *Organometallics*, 2012, **31**, 716–721.
130 J. J. Adams, N. Arulsamy and D. M. Roddick, Investigation of Iridium CF3PCP Pincer Catalytic Dehydrogenation and Decarbonylation Chemistry, *Organometallics*, 2012, **31**, 1439–1447.
131 E. P. K. Olsen and R. Madsen, Iridium-Catalyzed Dehydrogenative Decarbonylation of Primary Alcohols with the Liberation of Syngas, *Chem. Eur. J.*, 2012, **18**, 16023–16029.
132 E. P. K. Olsen, T. Singh, P. Harris, P. G. Andersson and R. Madsen, Experimental and Theoretical Mechanistic Investigation of the Iridium-Catalyzed Dehydrogenative Decarbonylation of Primary Alcohols, *J. Am. Chem. Soc.*, 2015, **137**, 834–842.
133 W. Jali, G. G. R. Green, S. J. Hart, A. C. Whitwood and S. B. Duckett, Iridium Cyclooctene Complex That Forms a Hyperpolarization Transfer Catalyst before Converting to a Binuclear C−H Bond Activation Product Responsible for Hydrogen Isotope Exchange, *Inorg. Chem.*, 2016, **55**, 11639–11643.
134 Y. Takahashi, M. Nonogawa, K. Fujita and R. Yamaguchi, C–H Activation on a Diphosphine and Hy-drido-Bridged Diiridium Complex: Generation and Detection of an Active IrII–IrII Species [(Cp*Ir)2(μ-dmpm)(μ-H)]+, *Dalt. Trans.*, 2008, 3546–3552.
135 F. A. Cotton and R. Poli, Ortho Metalation of Pyridine at a Diiridium Center. Synthesis and Spectroscopic and Crystallographic Characterization of NC5H4- and N,N’-Di-p-tolylformamidinato-Bridged Complexes of Diiridium(II), *Organometallics*, 1987, **6**, 1743–1751.
136 S. M. Kloek, D. M. Heinekey and k. I. Goldberg, Stereoselective Decarbonylation of Methanol to Form a Stable Iridium(III) trans-Dihydride Complex, *Organometallics*, 2006, **25**, 3007–3011.
137 B. L. Conley and T. J. Williams, Ligand-Metal Dual Site Catalysts for Hydride Manipulation, *Inorg. Chem.*, 2012, **32**, 195–218.
138 Z. Lu, B. Malinoski, A. V. Flores, B. L. Conley, D. Guess and T. J. Williams, Alcohol Dehydrogenation with a Dual Site Ruthenium, Boron Catalyst Occurs at Ruthenium, *Catalysts*, 2012, **2**, 412–421.
139 Z. Lu and T. J. Williams, A dual site catalyst for mild, selective nitrile reduction., *Chem. Commun. (Camb).*, 2014,

50, 5391–5393.

140 Z. Lu, B. L. Conley and T. J. Williams, A three-stage mechanistic model for ammonia-borane dehydrogenation by Shvo's catalyst, *Organometallics*, 2012, **31**, 6705–6714.

141 J. J. A. Celaje, X. Zhang, F. Zhang, L. Kam, J. R. Herron and T. J. Williams, A Base and Solvent-Free Ruthenium-Catalyzed Alkylation of Amines, *ACS Catal.*, 2017, **7**, 1136–1142.